Journal of Alloys and Compounds 500 (2010) 102–107

Contents lists available at ScienceDirect

Journal of Alloys and Compounds

journal homepage: www.elsevier.com/locate/jallcom

Effects of temperatures and cations of electrolyte on the capacitive characteristics of the manganese oxide deposited by hydrothermal electrochemical method

Chih-Hsiang Liang, Chii-Shyang Hwang*

Department of Materials Science and Engineering, Frontier Material and Micro/Nano Science and Technology Center, National Cheng Kung University, Tainan 70101, Taiwan

ARTICLE INFO

Article history:
Received 11 May 2009
Received in revised form 26 March 2010
Accepted 1 April 2010
Available online 7 April 2010

Keywords:
Electrode material
Oxide materials
Ionic conduction
Microstructure
Oxidation

ABSTRACT

A nanoscale hydrous manganese oxide used as an electrode in a supercapacitor was deposited onto a titanium substrate from an aqueous manganese acetate solution using the hydrothermal electrochemical method. The effect of deposition temperature on the characteristics of the manganese oxides was investigated. The capacitive characteristics of the manganese oxides were measured in sulfate electrolytes with various cations using cyclic voltammetry. The capacitive performances of the manganese oxide electrodes depend on the deposition temperature as well as the cations of electrolytes. A maximum capacitance of 244 F g^{-1} was obtained in Na_2SO_4 solution. The stability of manganese oxide was examined; after 1000 cycles, 80% of the initial capacitance remained.

1. Introduction

Supercapacitors have recently attracted a lot of interests for use as charge storage devices due to their quickly response, high power density, and long cycle life. It has been reported that supercapacitors with a ruthenium oxide electrode exhibit a large specific capacitance (SC) of as high as 750 F g^{-1} [1,2]. However, the high cost of ruthenium oxides and the use of toxic sulfuric acid as the electrolyte limit their commercial appeal. In order to reduce supercapacitor electrode material cost, activated carbons [3], transition metal oxides such as nickel oxide [4], ferric oxide [5], cobalt oxide [6], and vanadium oxide [7] have been studied as electrode material candidates. Manganese oxides have various oxidation states and excellent electrochemical performance [8–11], and have thus been considered as electrode materials. Manganese oxides have been prepared using various deposition methods, such as thermal decomposition [12], sol–gel methods [13], and electrochemical deposition [14–16]. The deposition method used to produce manganese oxides affects their characteristics, which in turn affect the performance of the manganese oxide electrodes. For example, porous morphologies and amorphous structures absorb more protons and cations in an aqueous electrolyte, and allow the ions to effectively utilize the electrode, producing higher SC [17,18]. In addition, a crystalline structure prevents manganese oxide from dissolving into the electrolyte during the charge/discharge test, which improves the stability for long-term applications [19]. In our previous studies, the hydrothermal electrochemical deposition (HED) method was used to deposit manganese oxides. In this deposition process, the hydrothermal reaction and electrochemical oxidation are combined to fabricate nanoscale amorphous or crystalline structures of manganese oxides [20–22].

Besides manganese oxide formations, the cations of the electrolyte affect SC when the electrode is immersed in the electrolyte during charge/discharge. Aqueous solutions, such as the electrolyte in a supercapacitor, produce high current flux due to the high conductivity of H^+ ions. Alkali ions, such as Na^+ and K^+, also attribute to capacitive performances; they were compared in various aqueous solutions using CV shapes in previous reports [23,24]. The results showed that the mobility of the ions in the electrolytic solution and the radius of the hydration sphere affect the CV performance. In our previous study, the concentration and operation temperature of the Na_2SO_4 electrolyte were studied; it was concluded that a concentration of 0.2 M and a temperature of 25 °C produced acceptable electrochemical behavior [25]. In the present study, the effects of deposition temperature and the cations of electrolytes on the capacitive behavior of manganese oxide electrodes in aqueous solution were investigated.

2. Experimental

Titanium foil (purity 99.7%), used as the working electrode substrate, was washed in distilled water and acetone for 10 min, and then dried at 105 °C in an oven for 10 min. A platinum wire and Ag/AgCl were used as the counter electrode and reference electrode, respectively. The electrodes were assembled into an autoclave pressure vessel (Parr 4571 reactor) to form a hydrothermal electrochemical

* Corresponding author.
E-mail address: cshwang@mail.ncku.edu.tw (C.-S. Hwang).

0925-8388/$ – see front matter.
doi:10.1016/j.jallcom.2010.04.001

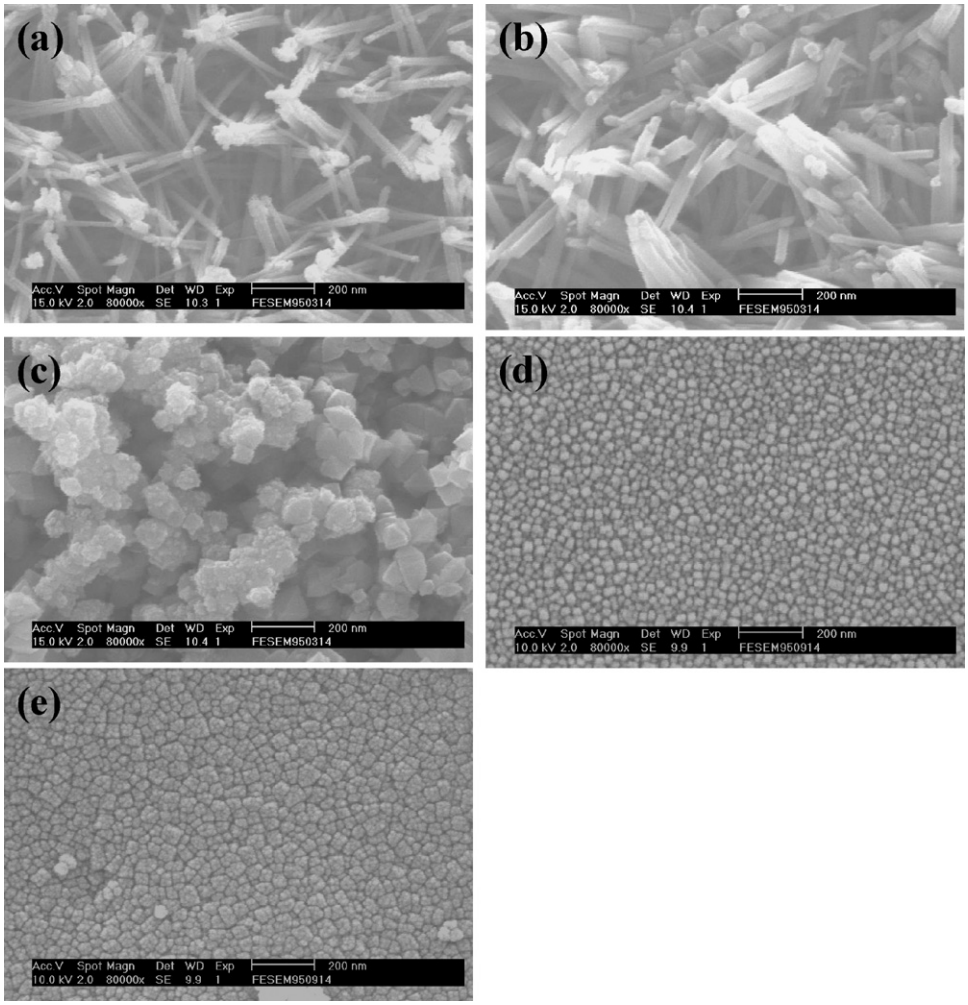

Fig. 1. FE-SEM images of manganese oxide films deposited at various temperatures: (a) 60, (b) 80, (c) 100, (d) 130, and (e) 150 °C.

cell. The area of the titanium substrate exposed to 0.2 M manganese acetate solution (Merck 99.0%) was $1.0 \times 1.0\,cm^2$. An automatic polarization potentiostat (Autolab/PGSTATA30) was employed. The potential was set to 0.8 V, which provided a total delivered charge of 0.5*C*. The weight of the as-grown deposits on the titanium substrate was estimated using a microbalance (Satorius CP225D) with an accuracy of 10 μg. The capacitive performance of as-grown electrodes was measured using a potentiostat (Autolab/PGSTAT30) at a constant scan rate of $20\,mV\,s^{-1}$ between 0 and 1 V in Na_2SO_4 (Merck 99.0%), K_2SO_4 (Merck 99.0%), $MgSO_4$ (Merck 99.5%), and Na_3PO_4 (Merck 98.0%) electrolytic solutions with a concentration of 0.1 M at a constant temperature of 25 °C. A cyclic-life test was conducted under these conditions for up to 1000 cycles.

The surface morphology of the manganese oxides was observed using a field-emission scanning electron microscope (FE-SEM, Philips XL-40FEG) and a transmission electron microscope (TEM, JEOL JSM-1200EX). The hydrous and oxidation states of the manganese oxides were examined using X-ray photoelectron spectroscopy (XPS) with a JEOL JPS-9010MX photoelectron spectrometer. The structure of the manganese oxides deposited at various temperatures was characterized using glancing-angle X-ray diffractometry (GAXRD, Panalytical X'Pert Pro). The patterns were recorded on a Moxtek PF2000 diffractometer at a glancing incident angle of 0.5°. The $K_{\alpha 1}$ radiation of a copper target with a wavelength of 1.54056 Å was used as the X-ray source.

3. Results and discussion

3.1. Microstructure of the manganese oxides

Fig. 1 shows the surface morphologies of the manganese oxides deposited at 60–150 °C using the HED method. The manganese oxides exhibited needle-like shapes that were tangled, forming a three-dimensional network. The width of the oxides increased from 15 to 20 nm when the deposition temperature was increased from 60 to 80 °C (Fig. 1(a) and (b)). When the temperature was increased to 100 °C, pores appeared and the needle-like manganese oxides agglomerated from the top to form coarse shapes 60 nm in width (Fig. 1(c)). The oxides grew to develop spherical particles that had compact and flat surface morphologies instead of individual particle formations when the temperature was increased to 130 and 150 °C (Fig. 1(d) and (e)). The manganese oxide shape thus depends on the deposition temperature. When the temperature exceeded 100 °C, the porous morphology transformed into a dense surface. The TEM image of the manganese oxide deposited at 60 °C shown in Fig. 2 was used to observe the oxide morphology in detail. The oxide structure was around 15 nm in width and 250 nm in length, and its aspect ratio was about 35. It is possible that the Mn^{2+} in the manganese acetate solution reacted with hydration to become manganese hydroxides on the titanium substrate, with other manganese hydroxides growing along the longitudinal direction to form needle-like structures. The manganese oxidation states were determined by calculating the multiplet splitting width of Mn 3s orbit peaks from the XPS spectra shown in Fig. 3 [26–28]. The peaks of XPS spectra shifted slightly to the left with increasing temperature. For the manganese oxides deposited at 60 °C, two distinct peaks located at 82.52 and 88.02 eV, respectively, were observed. The multiplet splitting width of manganese oxide deposited at various temperatures was calculated; the results are listed in Table 1. The peak separation (ΔE) of Mn 3s spectra decreased from 5.50 to 5.34 eV when the temperature was increased from 60 to 150 °C;

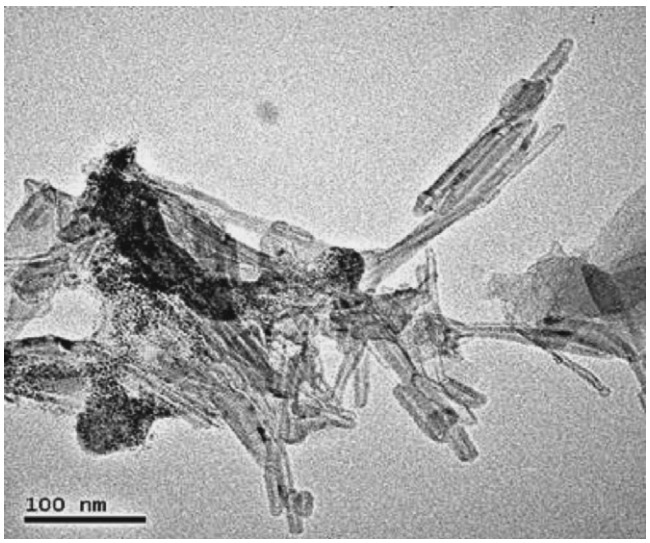

Fig. 2. TEM image of manganese oxide deposited at 60 °C.

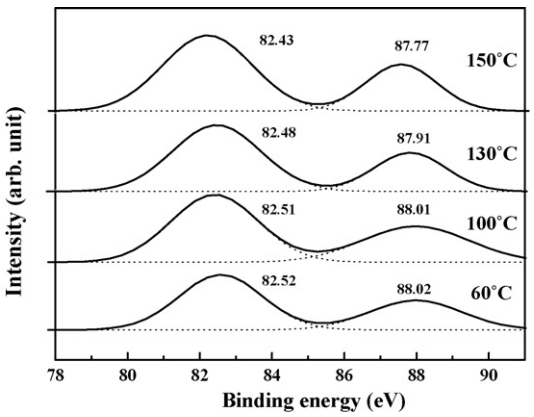

Fig. 3. XPS spectra of the Mn 3s region for manganese oxides deposited at various temperatures. Dotted lines show the mixed Gaussian component peaks.

however, all of the Mn oxidation states were both divalent and trivalent. This indicates that the manganese oxide states are independent of deposition temperature in the range 60–150 °C. The relative amount of hydration in the manganese oxide was also determined from the XPS spectra of the O1s orbit shown in Fig. 4. The main peak of O 1s, located at around 529 eV contributed to three peaks: Mn–O–Mn at 529.3–530.0 eV, Mn–O–H at 530.5–531.5 eV, and H–O–H at 531.8–532.8 eV [26–28]. The amount of hydration was 24.87% at 60 °C, and declined rapidly to 3.71% after the temperature was increased to 150 °C. The relative amounts of hydration are summarized in Table 1.

Table 1
XPS peak of Mn 3s and O 1s spectra results for manganese oxides deposited at various temperatures.

	Amount of hydration (%)	Eb1 (eV)	Eb2 (eV)	ΔE (eV)	Species [26–28]
60 °C	24.87	82.52	88.02	5.50	
100 °C	18.46	82.51	88.01	5.50	
130 °C	4.47	82.48	87.91	5.43	
150 °C	3.71	82.43	87.77	5.34	
				5.79–5.80	MnO
				5.30–5.50	Mn_3O_4
				5.20–5.41	Mn_2O_3
				4.70–4.78	MnO_2

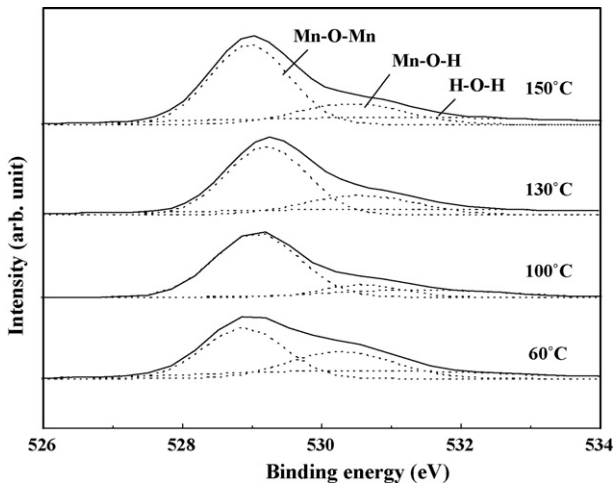

Fig. 4. XPS spectra of the O 1s region for manganese oxides deposited at various temperatures. Dotted lines show the mixed Gaussian component peaks.

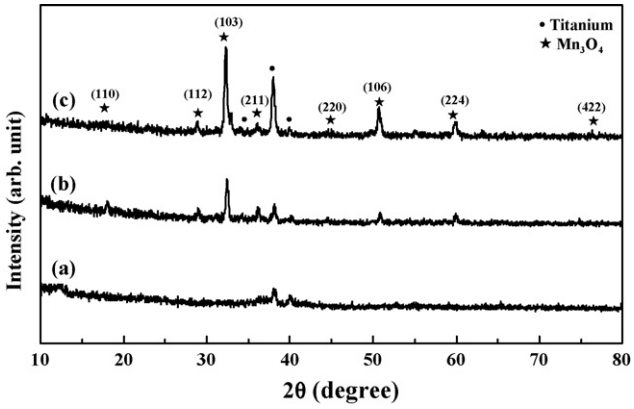

Fig. 5. XRD patterns of manganese oxides deposited at (a) 60, (b) 100, and (c) 150 °C.

Fig. 5 shows the XRD patterns of the manganese oxides deposited at 60, 100, and 150 °C. In addition to the diffraction peaks associated with the titanium substrate, peaks of crystalline hausmannite Mn_3O_4 were found. The manganese oxide deposited at 60 °C shows a broad and weak XRD peak, suggesting an amorphous or nanoscale oxide film. Distinct Mn_3O_4 peaks appeared when the temperature was increased to 100 °C. A crystalline nanoscale Mn_3O_4 structure was obtained at temperatures over 100 °C. Compared with other methods for synthesizing Mn_3O_4, such as cathodic electrosynthesis which includes heat treated for 1 h at 300 °C [16], the HED method is efficient.

3.2. Electrochemical behavior of manganese oxides

Fig. 6 shows the typical cyclic voltammetry (CV) curves for the manganese oxides deposited at temperatures from 60 to 150 °C measured in 0.1 M Na_2SO_4. Rectangular-like shapes that consisted of symmetric peaks can be seen for all curves. These symmetric rectangular-like curves indicate that the manganese oxides have good electrochemical reversibility and capacitive behavior between 0 and 1 V. The closed areas of CV curves decreased with increasing temperature. The SC of manganese oxides depends on these closed areas. The closed area represents the charges that manganese oxides store during the CV test. The relative SC values of manganese oxides deposited at 60, 80, 100, 130, and 150 °C were 244, 151, 126, 37, and 33 F g^{-1}, respectively. The protons in the aqueous solutions intercalated into the solid structures to reduce

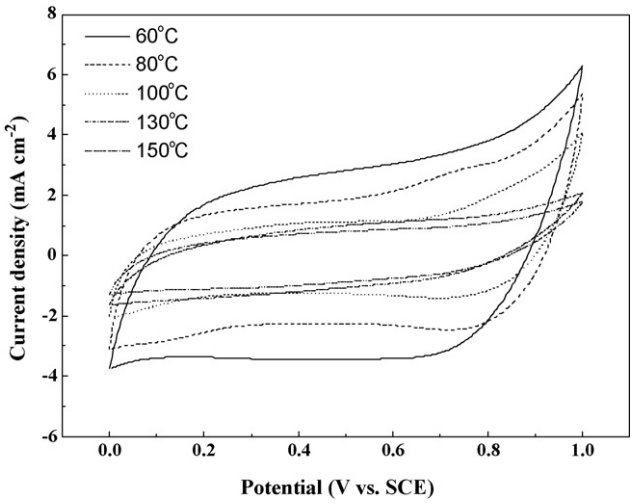

Fig. 6. Cyclic voltammetry curves of manganese oxides deposited at temperatures from 60 °C to 150 °C measured in Na_2SO_4 solution at a concentration of 0.1 M.

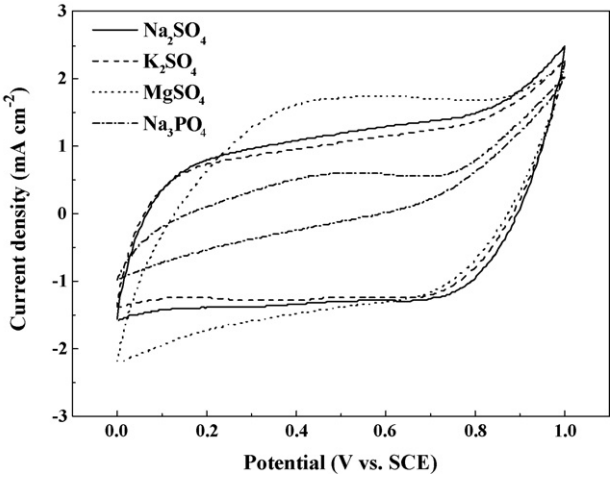

Fig. 7. Cyclic voltammerty curves of the manganese oxide deposited at 60 °C measured in various electrolytes at a concentration of 0.1 M at 25 °C.

MnOx during the charge/discharge cycles for SC measurements [29]. However, other reports have pointed out that alkali ions in the electrolytes might participate in the charge/discharge cycles to improve the SC [7,24]. Therefore, the reactions of MnO_x reduction can be expresses as:

$$MnO_x + \delta H^+ + \delta e^- \Leftrightarrow MnO_{x-\delta}(OH)_\delta \quad (1)$$

$$MnO_x + \delta M^+ + \delta e^- \Leftrightarrow M_\delta MnO_x \quad (2)$$

To investigate the effect of cations in the electrolytes on the capacitive performance, the manganese oxides deposited at a temperature of 60 °C were measured in Na_2SO_4, K_2SO_4, $MgSO_4$, and Na_3PO_4 solutions with a concentration of 0.1 M. The CV curves are shown in Fig. 7. In Na_2SO_4 and K_2SO_4 solutions, the CV curves exhibit similar rectangular shapes, indicating that the manganese oxides in both solutions had good capacitive characteristics. For the manganese oxides measured in $MgSO_4$ and Na_3PO_4 solutions; however, the CV curves did not have the acceptable shapes, meaning that neither is suitable as an electrolyte for this supercapacitor. The SC values of electrodes in Na_2SO_4, K_2SO_4, $MgSO_4$, and Na_3PO_4 solutions calculated from the CV curves were 242, 212, 284, and 115 $F g^{-1}$, respectively, as shown in Fig. 8. The SC measured in Na_2SO_4 solution had the smallest variation. According to these results, Na_2SO_4 as the electrolyte in the supercapacitor had stable

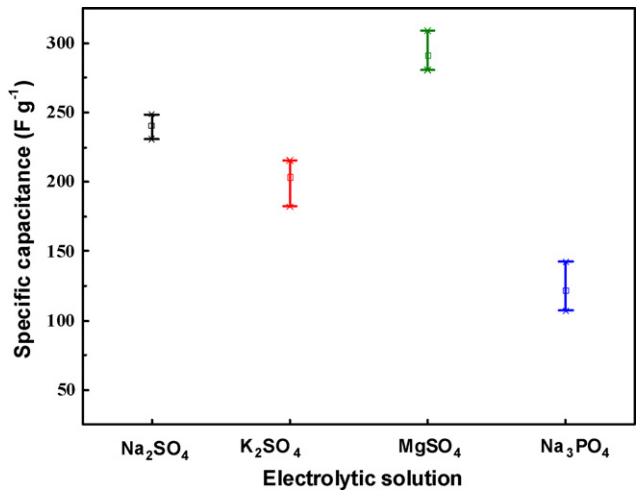

Fig. 8. Deviation of specific capacitance of manganese oxide electrodes deposited at 60 °C measured in various kinds of electrolyte at a concentration of 0.1 M at 25 °C.

Table 2
Conductivity and mobility of various cations in infinitely diluted aqueous solutions [31,32].

Cations	Conductivity (10^{-4} m^2 s mol^{-1})	Mobility (10^{-8} m^2 s V^{-1})
Na^+	50.1	5.19
K^+	73.5	7.62
$1/2Mg^{2+}$	53.1	2.75

Table 3
Radii of various cations in the aqueous solutions [31,32].

	Atomic radii (Å)	Ionic radii (Å)	Radii of hydration sphere (Å)
Na	1.80	1.02	3.58
K	2.20	1.38	3.31
Mg	1.50	0.72	4.28

SC. It was well known that SC is dominated by the accessible surface of manganese oxide for proton and electrolyte cation adsorption/desorption [18,30]. In addition to protons, suitable cations in the electrolyte improve capacitive performance, especially SC. It could be concluded that protons and suitable cations use the accessible surface of the manganese oxide electrodes to increase SC. The radii, conductivity, and mobility of various cations are listed in Tables 2 and 3. Mg^{2+} had more charges than do Na^+ and K^+ in the solution and showed higher SC, but its mobility and hydration sphere radius were negative characters, especially the hydration sphere radius, making it difficult to insert into the manganese oxides to retard the charge/discharge response. The effect of the Mg^{2+} hydration sphere radius can be observed on the CV curve for manganese oxide measured in the $MgSO_4$ solution (Fig. 7). K^+ had the best mobility, conductivity, and hydration sphere radius; however, a large variation of SC made the electric output unstable. Na_3PO_4 had poor performance in the CV curve because it could not dissolve completely in the solution; thus, there were insufficient cations to carry charges to improve SC. The capacitive stability of as-deposited manganese oxide was demonstrated in various electrolytic solutions with long operation tests for up to 1000 cycles. Fig. 9 shows the variation of SC as a function of the number of cycles. The decay rates of SC measured in Na_2SO_4, K_2SO_4, $MgSO_4$, and Na_3PO_4 solutions after 1000 cycles were around 20%, 23%, 33%, and 86%, respectively. The SC of manganese oxide measured in various electrolytes decreased significantly during the first 200 cycles and remained at a constant value after 700 cycles. Although the

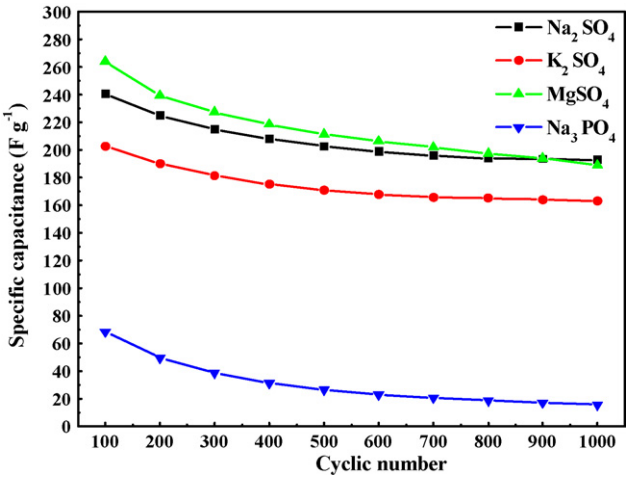

Fig. 9. Specific capacitance of manganese oxides as a function of the number of cycles measured in various electrolytes at a concentration of 0.1 M at 25 °C.

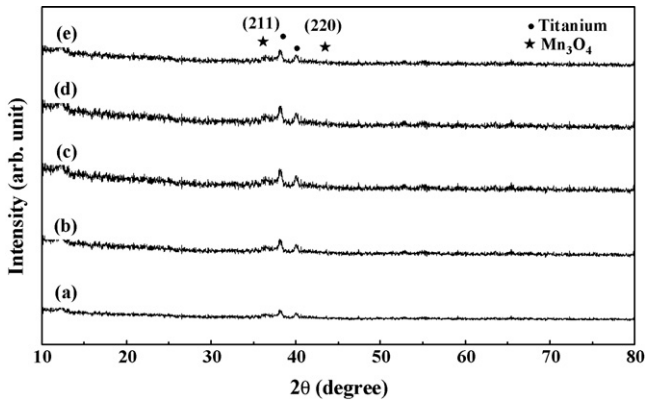

Fig. 11. X-ray diffraction patterns of manganese oxides deposited at 60 °C measured (a) before the 1000-cycle test in 0.1 M of Na_2SO_4 and after 1000 cycles in (b) Na_2SO_4, (c) K_2SO_4, (d) $MgSO_4$, and (e) Na_3PO_4.

initial SC of manganese oxide measured in $MgSO_4$ had the highest value of 284 F g^{-1}, the decay rate of SC increased rapidly after 1000 cycles. In contrast, manganese oxide in Na_2SO_4 and K_2SO_4 showed smooth SC fading curves with increasing number of cycles. For larger variation of SC when used as the electrolyte, Na_2SO_4 as the electrolyte not only presented acceptable SC, but also showed the distinguished capacitive stability.

The surface morphologies of manganese oxides deposited at 60 °C measured in 0.1 M of various electrolytic solutions after 1000 cycles are shown in Fig. 10. For the manganese oxide deposited at 60 °C, the morphology changed from needle-like (Fig. 1(a)) to leaf-like shapes excluding oxides measured in Na_3PO_4 solution (Fig. 10(d)). The leaf-like shape consisted of a thin membrane between needle-shaped oxides, and had many pores. The morphology of the manganese oxide measured in Na_3PO_4 solution consisted of thin needle shapes that formed a strand which reduced the surface area and thus lowered SC performance.

The XRD patterns of manganese oxide deposited at 60 °C measured in 0.1 M of various electrolytes after 1000 cycles are shown in Fig. 11. Crystalline hausmannite Mn_3O_4 peaks were observed for all electrolytes. The manganese oxide structures changed from amorphous to crystalline after the charge/discharge operation. Although an amorphous structure allowed protons and cations to easily adsorb/desorb into the electrode improving SC, the SC significantly dropped after many cycles. In contrast, the solid crystalline structure prevented manganese oxides from dissolving into the electrolyte, and thus improved the capacitive stability.

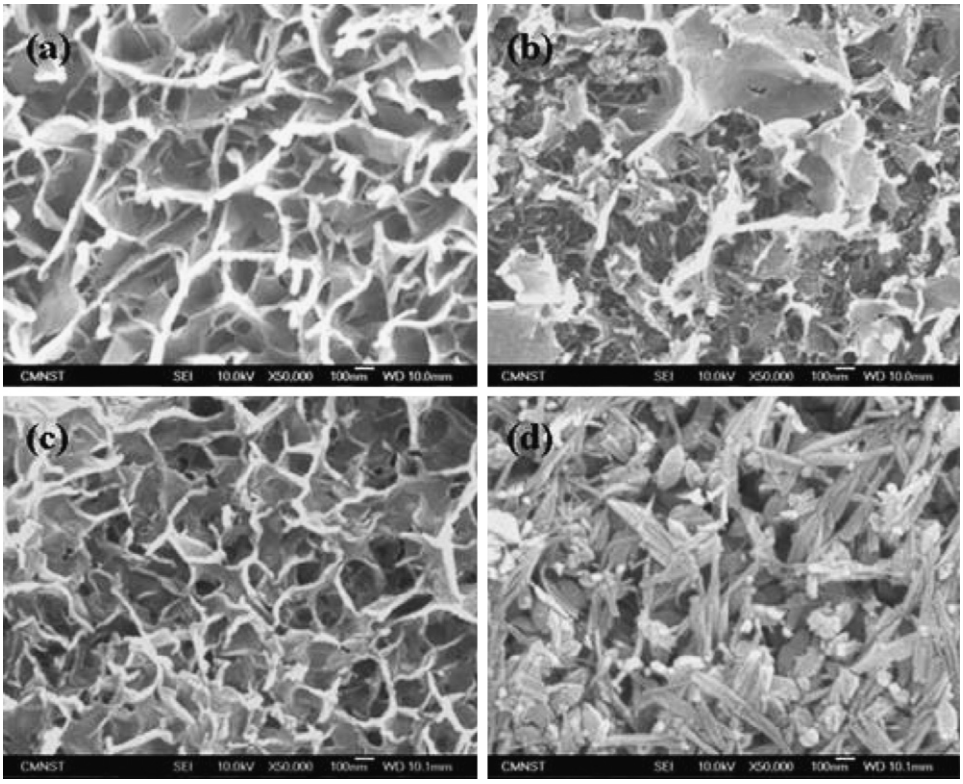

Fig. 10. Surface morphologies of manganese oxide electrodes deposited at 60 °C after 1000 cycles measured in 0.1 M of (a) Na_2SO_4, (b) K_2SO_4, (c) $MgSO_4$, and (d) Na_3PO_4.

4. Conclusions

In the present study, a nanoscale hydrous manganese oxide was deposited onto a titanium substrate from manganese acetate solution with a concentration of 0.2 M using the HED method. Various deposition temperatures ranging from 60 to 150 °C were applied to deposit the manganese oxides as a supercapacitor electrode. Needle-like structures formed at a deposition temperature of 60 °C. The manganese oxide became coarse, showing a compact and flat surface, when the deposition temperature was increased to 150 °C. In addition, the oxidation states of manganese were divalent and trivalent for deposition temperatures ranging from 60 to 150 °C. Crystalline Mn_3O_4 peaks appeared for deposition temperatures of over 100 °C. The capacitive behavior and electrochemical characteristics were evaluated in sulfate electrolytes with various cations using the CV test. Na_2SO_4 as the supercapacitor electrolyte had an acceptable SC of 242 F g^{-1} and capacitive stability; its decay rate of SC after 1000 charge/discharge cycles was around 20%. The manganese oxide transformed into crystalline structures after being subjected to the charge/discharge cycle test.

Acknowledgements

The authors would like to thank the National Science Council of the Republic of China, Taiwan, for financially supporting this research under grant NSC95-2221-E-006-189 and the NCKU Project of Promoting Academic Excellence & Developing World Class Research Center (D96-2700). The authors would also like to thank the Center for Micro/Nano Technology Research, National Cheng Kung University, Tainan, Taiwan, for equipment access and technical support.

References

[1] J.P. Zheng, P.J. Cygon, T.R. Jow, J. Electrochem. Soc. 142 (1995) 2699–2703.
[2] C.C. Hu, Y.H. Huang, J. Electrochem. Soc. 146 (1999) 2465–2471.
[3] J.P. Zheng, J. Huang, T.R. Jow, J. Electrochem. Soc. 144 (1997) 2417–2420.
[4] K.C. Liu, M.A. Anderson, J. Electrochem. Soc. 143 (1996) 124–130.
[5] N.L. Wu, S.Y. Wang, C.Y. Han, D.S. Wu, L.R. Shiue, J. Power Sources 113 (2003) 173–178.
[6] C. Lin, J.A. Ritter, B.N. Popov, J. Electrochem. Soc. 145 (1998) 4097–4103.
[7] H.Y. Lee, J.B. Goodenough, J. Solid State Chem. 148 (1999) 81–84.
[8] J.P. Zheng, J. Huang, T.R. Jow, J. Electrochem. Soc. 144 (1997) 2026–2031.
[9] B.E. Conway, J. Electrochem. Soc. 138 (1991) 1539–1548.
[10] J.K. Chang, W.T. Tsai, J. Electrochem. Soc. 150 (2003) A1333–A1338.
[11] D. Waldbillig, A. Wood, D.G. Ivey, J. Power Sources 145 (2005) 206–215.
[12] H.Y. Lee, V. Manivannan, J.B. Goodenough, Comptes Rendus Chimie 2 (1999) 565–577.
[13] S.C. Pang, M.A. Anderson, T.W. Chapman, J. Electrochem. Soc. 147 (2000) 444–450.
[14] J.K. Chang, M.T. Lee, W.T. Tsai, J. Power Sources 166 (2007) 590–594.
[15] C.C. Hu, T.W. Tsou, Electrochim. Acta 47 (2002) 3523–3532.
[16] N. Nagarajan, H. Humadi, I. Zhitomirsky, Electrochim. Acta 51 (2006) 3039–3045.
[17] B. E. Conway, Ionic Hydration in Chemistry and Biophysics, Elsevier, Amsterdam (1981).
[18] J.N. Broughton, M.J. Brett, Electrochim. Acta 50 (2005) 4814–4819.
[19] R.N. Reddy, R.G. Reddy, J. Power Sources 124 (2003) 330–337.
[20] C.H. Liang, C.S. Hwang, M. Yoshimura, J. Ceram. Soc. Jpn. 115 (2007) 349–353.
[21] C.H. Liang, C.S. Hwang, Jpn. J. Appl. Phys. 47 (2008) 1662–1666.
[22] C.H. Liang, C.S. Hwang, Jpn. J. Appl. Phys. 47 (2008) 4682–4686.
[23] S. Wen, J.W. Lee, I.H. Yeo, J. Park, S.I. Mho, Electrochim. Acta 50 (2004) 849–855.
[24] H.Y. Lee, J.B. Goodenough, J. Solid State Chem. 144 (1999) 220–223.
[25] C.H. Liang, C.S. Hwang, J. Ceram. Soc. Jpn. 115 (2007) 319–323.
[26] M. Chigane, M. Ishikawa, M. Izaki, J. Electrochem. Soc. 148 (2001) D96–D101.
[27] M. Chigane, M. Ishikawa, J. Electrochem. Soc. 147 (2000) 2246–2251.
[28] B. Djurfors, J.N. Broughton, M.J. Brett, D.G. Ivey, J. Electrochem. Soc. 153 (2006) A64–A68.
[29] C.C. Hu, T.W. Tsou, J. Power Sources 115 (2003) 179–186.
[30] M. Wu, L. Zhang, J. Gao, C. Xiao, D. Wang, A. Chen, S. Zhang, J. Electroanal. Chem. 613 (2008) 125–130.
[31] H. Joseph, Noggle, Physical Chemistry, second ed., Scott Foresman and Coppany, Glenview, IL, 1989.
[32] Y. Marcus, Ion properties, Marcel Dekker, New York, 1997.